Hydration of Sodium(I) and Potassium(I) Revisited: A Comparative QM/MM and QMCF MD Simulation Study of Weakly Hydrated Ions

S. Sikander Azam, Thomas S. Hofer, Bernhard R. Randolf, and Bernd M. Rode*

Theoretical Chemistry Division Institute of General, Inorganic and Theoretical Chemistry University of Innsbruck, Innrain 52a, A-6020 Innsbruck, Austria

Received: October 22, 2008; Revised Manuscript Received: December 9, 2008

Quantum mechanical/molecular mechanical (QM/MM) and quantum mechanical charge field (QMCF) molecular (MD) simulations have been performed to describe structural and dynamical properties of Na(I) and K(I) in water and to compare the two approaches. The first and second hydration shells were treated by ab initio quantum mechanics at the restricted Hartree−Fock (RHF) level. The structural data are in good agreement with previously published experimental and theoretical results. A considerable number of water exchange reactions were observed within the first shell during the simulation time of 12 ps. The number of exchange events in both shells is higher in the case of K(I) than Na(I) reflecting the weaker ion−ligand bond strength of K(I). Comparison of the "conventional" QM/MM framework with the QMCF method clearly indicates the latter to be advantageous, as ambiguities arising from the coupling of the subregions occurring in the QM/MM MD simulations did not evolve when the QMCF ansatz was applied.

1. Introduction

Inspite of the available description of metal ions and their manifold applications, detailed knowledge of their behavior has always been desirable in order to obtain insight of the crucial role they play in biochemistry and pharmacology.[1,2] Deficiencies of Na^+ or K^+ in mammals result in various disorders such as deafness, imbalance,[3] cardiac arrhythmia, bone disorders, and other ion channel diseases.[4] The presence of sodium and potassium ions in cytoplasm and their key role in everyday cell operation and regulation make them a topic of extensive research. These ions are tightly connected to the functions of Na−K pumps, which maintain homostasis, control nerve, and muscle functions as well as osmosis in cells and blood. The role of these ions in pathophysiology of hypertension[5] and in various biochemical phenomena is also unambigous.[4] In a recent research hyponatremia is identified as a risk factor for increased morbidity and mortality in patients of congestive heart failure while potassium maintains electrical activity inside the heart.[6,7] Deficiency of potassium leads to cell bursts and other cardiological disorders. In addition to their biochemical importance they are equally useful in industry. In light of all these facts, the importance of these ions is obvious and a large number of experiments and theoretical investigations have been carried out.[8−21] The ion induced modification to the structure of water is currently addressed by interpreting neutron diffraction data from monovalent ionic solutions of NaCl and KCl using computer assisted structural modeling techniques.[22] Recent findings indicated that the hydration of both ions must involve significant disruption to the water network, with highly bent or broken hydrogen bonds,[23] which resolves the vibrant debate on the range of statements on the effect of ions perturbing the local structure of water and concepts of ions being "structure makers" or "structure breakers".[22] Results obtained from computer simulation yield detailed insight into structure and dynamics at the molecular level allowing the interpretation of experimental observations. Ongoing developments in computational capacities open up the way to utilize more sophisticated simulation techniques using combined quantum mechanical and molecular mechanical (QM/MM) simulations.[24−28] The recently developed quantum mechancial charge field (QMCF) approach for general treatment of solvated systems further enhances the capabilities of this methodology.[29,30] The present work aims at yielding detailed insight into the structure and dynamics of Na(I) and K(I), at the same time comparing the performance of QM/MM MD simulations commonly used for solvated ions and the recently formulated QMCF MD approach.

2. Methods

When performing quantum chemical studies one of the most crucial steps is the selection of suitable basis sets. The LANL2DZ basis sets were selected since ab initio geometry optimizations using these basis sets reproduce structural properties rather well with respect to calculations using larger basis sets according to previous investigations and test calculations performed by Tongraar et al.[31] For O and H Dunning double-ζ plus polarization basis sets were employed.[31] The choice of a proper quantum mechanical level for the calculation is also an essential factor in determining the accuracy, computation time, and also the quantitative correctness of QM/MM results. Previous QM/MM and QMCF MD simulations of ionic solutes[32,33] have yielded data in good agreement with experimental measurements if the ab initio Hartree−Fock (HF) method utilizing at least double-ζ plus polarization basis sets was employed. Despite their common popularity, density functional methods (DFT) yielded results different from experimental data[34−36] as well as from correlated ab initio methods[34,37−43] for ion−water systems. To estimate the reliability of our method of choice, geometry optimizations of Na^+ and K^+ clusters with 1−6 water molecules were performed at different levels of theory. The corresponding ion−oxygen distances according to the methods HF, MP2, B3LYP, and CCSD are presented in Table 1. In the case of K(I) these values indicate that there are almost identical K−O distances when applying HF, CCSD, and MP2 to the various

* Corresponding author. E-mail: bernd.m.rode@uibk.ac.at. Phone: +43-512-507-5129. Fax: +43-512-507-2714.

10.1021/jp8093462 CCC: $40.75
Published on Web 02/09/2009

TABLE 1: Average K−O and Na−O distances (in Å) for K(I)−$(H_2O)_n$ and Na(I)−$(H_2O)_n$ Clusters Obtained from HF, CCSD, MP2, and B3LYP Calculations

n	HF	CCSD	MP2	B3LYP
		r_{K-O} in Å		
1	2.69	2.69	2.69	2.65
2	2.71	2.72	2.71	2.67
3	2.73	2.73	2.73	2.69
4	2.76	2.76	2.76	2.71
6	2.85	2.84	2.84	2.80
		r_{Na-O} in Å		
1	2.28	2.29	2.29	2.27
2	2.29	2.30	2.30	2.82
3	2.32	2.32	2.32	2.30
4	2.35	2.35	2.35	2.35
6	2.46	2.45	2.45	2.44

hydrated clusters. B3LYP delivers considerably shorter distances thus making this method less favorable in this case. For Na(I), the distances are found to be quite insensitive to the method applied, although B3LYP gives again slightly shorter bonds. Considering these results and the experience obtained from previous studies the HF level appears to be the best compromise between accuracy and computational effort.

In QM/MM approaches[24−28] the system is divided into two parts, thereby treating the chemically most relevant region, the ion and its immediate vicinity, by ab initio quantum mechanics while the remaining part of the system is accounted for by empirical potentials. The coupling between the QM and MM regions is also based on potential functions. In most cases ab initio generated pair potentials representing the interactions between particles in the QM region and molecules in the MM zone are utilized. The construction of these potential functions is a difficult and time-consuming task. To resolve these problems an improved methodology, the QMCF framework, has been formulated[29,30] that does not require any non-Coloumbic interaction potentials between solute and solvent particles. The radius of the QM region is enlarged to distances after which non-Coloumbic contributions between solute and solvent molecules are negligibly small and the only contribution results from the Coulombic interactions. Obviously, this requirement is violated for particles located near the QM/MM interface, hence in addition to the Coulombic terms non-Coulombic potentials have to be applied for those particles. If only solvent molecules are allowed in this region, this does not pose any problems as a large number of suitable solvent potentials are available in the literature. The interactions between particles located in the MM region are treated by application of the chosen force field method. According to the discussed treatment of forces the QM region is further split into two subregions for coupling purposes: the "core" region (inner QM subregion) containing the solute and its immediate ligands and the "solvation layer" (outer QM subregion) composed of at least one shell of solvent molecules (cf. Figure 1). Thus, the QMCF framwork offers a straighforward route to access any kind of solutes such as metal complexes and even composite solute species.[44,45]

The forces acting on particles in the different subregions are derived according to the following equations:

$$\vec{F}_J^{\text{core}} = \vec{F}_J^{\text{QM}} + \sum_{I=1}^{N_1+N_2} \frac{q_I^{\text{QM}} \cdot q_J^{\text{MM}}}{\vec{r}_{IJ}^{\,2}} \tag{1}$$

$$\vec{F}_J^{\text{layer}} = \vec{F}_J^{\text{QM}} + \sum_{I=1}^{M} \vec{F}_{IJ}^{\text{BJHnC}} + \sum_{I=1}^{N_1+N_2} \frac{q_I^{\text{QM}} \cdot q_J^{\text{MM}}}{\vec{r}_{IJ}^{\,2}} \tag{2}$$

$$\vec{F}_J^{\text{MM}} = \sum_{\substack{I=1 \\ I\neq J}}^{M} \vec{F}_{IJ}^{\text{BJH}} + \sum_{I=1}^{N_1+N_2} \frac{q_I^{\text{QM}} \cdot q_J^{\text{MM}}}{\vec{r}_{IJ}^{\,2}} + \sum_{I=1}^{N_2} \vec{F}_{IJ}^{\text{BJHnC}} \tag{3}$$

F_J^{core} (eq 1) corresponds to the quantum mechanical forces acting on a particle J in the core zone, F_J^{layer} to the forces acting on a particle J located in the solvation layer, and F_J^{MM} to the forces acting on a particle J in the MM region. The forces in the core region are obtained from the quantum mechanical treatment plus the Coulombic forces resulting from all MM atoms. The partial charges of the quantum mechanical particles are derived via population analysis in every subsequent step of the simulation. This treatment was found to be preferred over the assignment of fixed charges as it includes effects resulting from charge transfer, many-body interactions and polarization as well as the influence of geometrical changes in the QM region. As partial charge schemes are in general sensitive to the chosen theoretical accuracy level and basis sets, test computations have to be performed prior to the simulation. The Mulliken population analysis scheme has been found to yield partial charges which are compatible to the charges of the BJH-CF2 model describing the solvent−solvent interaction in the MM region. For particles in the solvation layer the non-Coulombic interactions of atoms with the MM particles obtained from the BJH-CF2 water model[46,47] are also taken into account, as this layer is in the immediate neighborhood of the MM region. The MM forces are composed of the forces resulting from the BJH-CF2 water model[46,47] plus the Coulombic forces exerted by all atoms present in the core region (N_1) and solvation layer (N_2) and the non-Coulombic forces resulting from the interaction with all atoms present in the solvation layer (N_2) (eq 3). According to these definitions all interactions are treated appropriately and the conservation of the linear momentum is ensured as the sum of forces equals zero.

To polarize the QM region due to the surrounding bulk of solvent molecules the point charges of the MM atoms are included as a perturbation term in the core Hamilton operator during the SCF procedure (eq 4):

$$\hat{H}_{CF} = \hat{H}_{HF} + \hat{V}' \tag{4}$$

$$\hat{V}' = \sum_{J=1}^{M} \frac{q_J}{r_{iJ}} \tag{5}$$

where q_J is the partial charge of the Jth particle of the M particles in the MM region. Without this electrostatic embedding the QM treatment is unaware of its surrounding and tends to relax toward a gas phase structure, and artifacts near the QM/MM interface could result.

Similar to the QM/MM approach,[8] an interval of 0.2 Å at the QM/MM border is utilized to ensure a smooth transition of migrating solvent molecules. The forces of the respective particles are evaluated twice, once as a QM particle and additionally as if the particle were already part of the *MM* region:

$$F_j^{\text{Smooth}} = S(r) \cdot (F_j^{\text{layer}} - F_j^{\text{MM}}) + F_j^{\text{MM}} \tag{6}$$

where the smoothing factor $S(r)$ is:

$$S(r) = 1, \quad \text{for } r \le r_1$$

$$S(r) = \frac{(r_0^2 - r^2)^2(r_0^2 + 2r^2 - 3r_1^2)}{(r_0^2 - r_1^2)^3}, \quad \text{for } r_1 < r \le r_0$$

$$S(r) = 0, \quad \text{for } r > r_0 \tag{7}$$

where r is the distance of a given solvent molecule's center of mass from the center of the QM region, r_0 is the radius of the

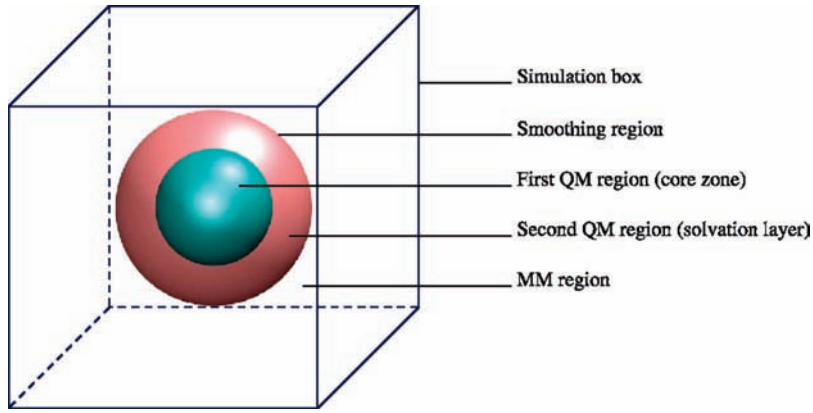

Figure 1. Partitioning of the simulation box in the QMCF approach.

QM region, and r_1 is the inner border of the smoothing region. A thickness of 0.2 Å is usually employed as this value was found to be the optimal distance to ensure smooth transitions. As smoothing takes place at a relatively large distance to the solute, transitions are less abrupt than in QM/MM procedures with smaller QM region, also because the influence of the MM region on the layer part of the QM region is fully included within the QMCF formalism. However, this procedure still leads to slight inconsistencies of the conservation of momentum as pointed out by Truhlar et al.,[24] but considering the small size of the smoothing region and the limited simulation time achievable in QMCF MD simulations, this error remains minor.

Radial and angular distribution functions were employed to characterize the structural properties of the complexes in aqueous solution. Mean ligand residence times (MRT, τ) for the first/second hydration shell were calculated by using the direct method.[48] The parameter t^*, determining the minimum time span to account for a ligand displacement from its original coordination shell, was set to 0.0 and 0.5 ps, respectively. The sustainability of exchange processes can be defined as:

$$S_{ex} = \frac{N_{ex}^{0.5}}{N_{ex}^{0}} \tag{8}$$

where S_{ex} is the sustainability coefficient, N_{ex}^{0} is the number of all transitions through a shell boundary ($t^* = 0.0$), and $N_{ex}^{0.5}$ denotes the number of exchanges persisting longer than 0.5 ps. Its inverse (R_{ex}) counts how many attempts are on average required to produce one lasting exchange between the hydration shells.

2.1. Simulation Protocol. A pre-equilibrated elementary cubic box with a side length of 24.6 Å containing one ion immersed in 499 water molecules was utilized as the starting structure. The density of the system corresponds to the pure solvent at 298 K (0.997 g/cm ^{3}). Periodic boundary conditions were applied and the canonical ensemble was chosen, whose temperature was controlled by the Berendsen algorithm.[49] A predictor−corrector algorithm was used to integrate the Newtonian equations of motion; the chosen time step was 0.2 fs. The cutoff distances for non-Coulombic interactions were set to 5.0 and 3.0 Å respectively for O−H and H−H interactions. For the Coulombic interactions a cutoff of 12.0 Å was set. The reaction field method was used to correct the errors associated with this cutoff. For water, the flexible BJH-CF2[46,47] potential was employed, as its intramolecular term ensures the full flexibility of water molecules necessary for a suitable transition from the QM into the MM region and vice versa. This flexibility also allows intramolecular vibrations and relaxation processes and thus the evaluation of vibrational spectra of the ligand molecules. Both QM/MM and QMCF MD simulations were performed by using the equilibrium configuration obtained from a preliminary QM/MM MD simulation including the ion and its first hydration shell into the QM region. All simulations were sampled for 12 ps after 5 ps of equilibration, respectively. The total radius of the QM region was set to 5.7 and 6.0 Å for Na(I) and K(I), respectively. In the case of the QMCF simulation the radius determining the core region was set to 3.0 and 3.5 Å in the cases of Na(I) and K(I), respectively.

3. Results and Discussion

Figure 2 displays a comparison of the ion−O and ion−H radial distribution functions (RDF) obtained from the QMCF and QM/MM MD simulations of Na(I) and K(I), respectively; the structural data are summarized in Table 2. The ion-oxygen radial distribution functions reveal well-defined first hydration shells. A faint indication of preferential orientation beyond the first shell can be detected; however, due to the very low intensities the presence of a distinct second hydration layer is ambiguous.

The most pronounced differences between the two approaches are found near the QM/MM transition region in the case of Na(I). The density in the region about 4.0 to 5.0 Å is clearly shifted toward larger distances upon application of the QMCF method, whereas intensity and integration (i.e., the coordination number; Figure 2) remains unchanged. Furthermore, the QM/MM framework leads to an increased intensity in the region between 6.0 and 7.0 Å, which is also visible in the Na−H RDF. This region clearly corresponds to bulk if the QMCF approach is applied. The higher intensity of the first shell peaks of the ion−H RDFs resulting from the QM/MM MD treatment appears noteworthy, as it indicates a better structurization of the hydrate.

The increased intensity as well as the shift of the second hydration shell in the vicinity of the QM/MM interface is the result of an artificial "pressure" of the MM molecules on the QM region in the "classical" QM/MM method. The Coulombic interactions of the QM/MM coupling are computed utilizing fixed charges for both QM and MM atoms, which do not take polarization effects and the corresponding change of the partial charges in the QM region into account. The formal charge of +1.0 assigned to the ion results in a too strong attraction of MM oxygens, leading to an increase of the water population in the region between 6.0 and 7.0 Å. This increased population exhibits a too strong repulsion, an artificial "pressure", on adjacent atoms located in the QM region (in this case the second hydration shell), which are forced to move toward the QM

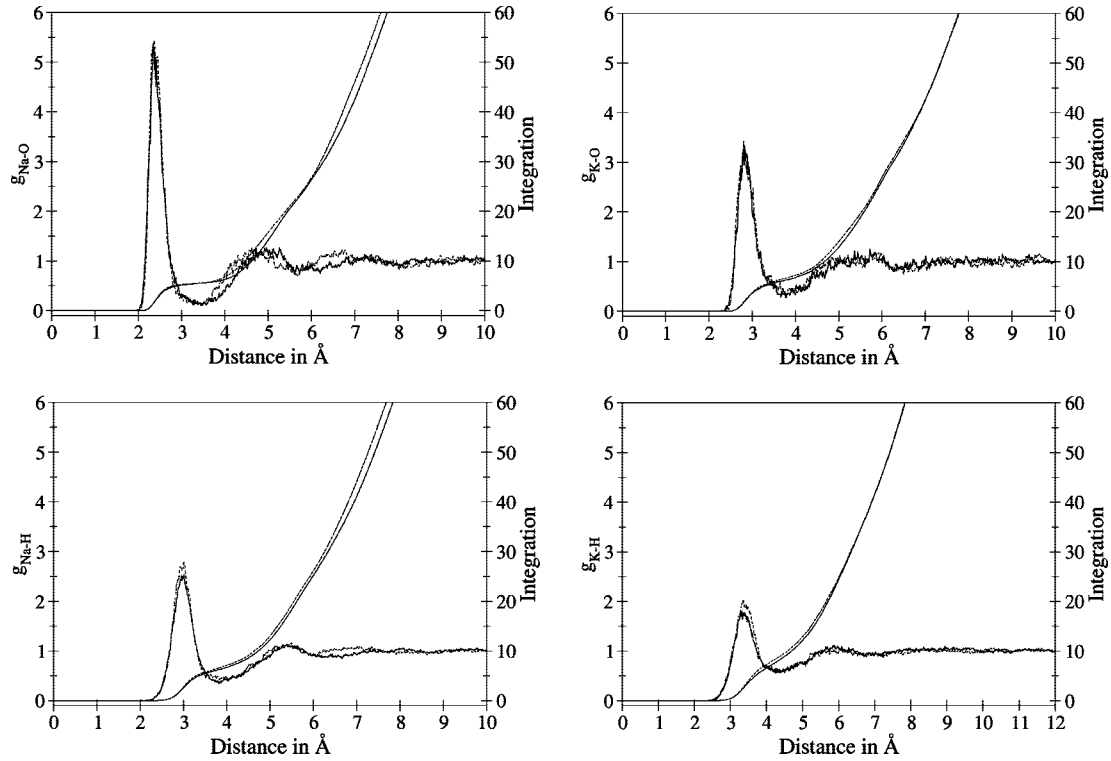

Figure 2. Comparison of the ion−water radial distribution functions for Na(I) and K(I) obtained from a QMCF (solid line) and a QM/MM MD simulation (dashed line).

TABLE 2: Maxima r_{max} and Minima r_{min} (in Å) for M(I)−O Distances and Respective Coordination Numbers (CNs) of First Hydration Shells Obtained from Theory and Experiment: Comparison of Hydration Parameters for Na(I) and K(I)

solute	concn	method	r_{max}	r_{min}	CN	ref
Na^+	1/199	CF2-water MD	2.36	3.04	6.5	31
	1/199	two-shell QM/MM MD	2.33	2.94	5.6	31
$NaNO_3$	6.01 M	XD	2.44		6	17
	3.13 M	XD	2.40		4.9	19
NaCl	2.0 M	XD	2.42		4.7	16
	1/499	two-shell QM/MM MD	2.36	3.45	5.5	this work
	1/499	two-shell QMCF MD	2.34	3.46	5.5	this work
K^+	1/199	CF2-water MD	2.78	3.40	7.8	31
	1/199	two-shell QM/MM MD	2.81	3.72	8.3	31
KCl	2.0M	XD	2.8		6	16
	4.0M	ND	3.1			18
	1/499	two-shell QM/MM MD	2.80	3.79	6.2	this work
	1/499	two-shell QMCF MD	2.80	3.77	6.8	this work

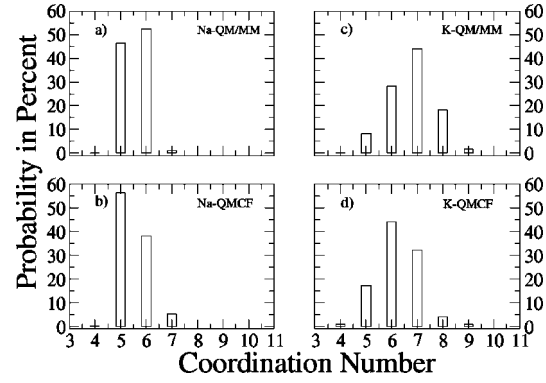

Figure 3. First shell coordination number distributions for Na(I) and K(I) obtained via a QMCF and a QM/MM MD simulation.

center. These data lead to similar conclusions as previous studies comparing the QM/MM and QMCF approaches.[50] On the other hand, the K(I)−water RDFs do not show any significant differences. This can be explained by the higher first shell coordination number and the weaker ion−solvent interactions. The increased number of ligands effectively shield the charge of the ion and thus no artificial behavior is observed.

The Na−O RDF indicates a flexible first shell with its maximum located at 2.36 and 2.34 Å obtained from the QM/MM and QMCF MD simulation, respectively. Integration up to the minima following the first shell (3.45 and 3.46 Å, respectively) yields an average first shell coordination number (CN) of 5.5 for QM/MM and QMCF MD simulations, suggesting that 5- and 6-fold coordination dominate. These values lie within the range of several experimental investigations (see Table 2 for comparison). The nonzero minima following the first shell peak indicate rapid ligand exchanges to and from the first hydration shell. This rapid solvent exchange in combination with the average coordination number of 5.5 also supplies a reasonable explanation for the relatively short Na−O distance of 2.34 Å resulting from the QMCF simulation: for experimental structures, where the ion is 5-coordinated, a very similar value of 2.34 to 2.40 Å was reported, whereas for 6-coordinated structures this value varies from 2.36 to 2.48 Å. In solution, the hydrate structure is apparently not only very labile, but also unsymmetric due to the rapid exchange, and the 5-coordinated and a distorted 6-coordinated structure are dominating the average composition, both with a relatively short Na−O distance.

Only a faint indication of a second shell is visible in the case of Na(I), the corresponding maxima are difficult to locate in the Na−O RDF and can be given as 4.6 and 5.0 Å for the QM/MM and the QMCF MD simulations, respectively. Similarly the minima indicating the borderline between second shell and bulk are difficult to identify, and they have been assigned as approximately 5.7 Å for the QM/MM and 5.6 Å for the QMCF study. Integration yields average coordination numbers

of 17.2 and 16.2. Considering the intensities of the Na−O RDF for minima between second shell minima and bulk (0.7 and 0.8, respectively), the influence of the ion beyond the first hydration layer is definitely very weak. These findings lead to the conclusion that only a single layer of hydration is formed.

The same conclusion can be drawn for the hydrated K(I) ion, for which the above-mentioned characteristics are even more pronounced. The first hydration shell is almost identically reproduced by both methods yielding an average K(I)−O distance of 2.8 Å. Integration of the K(I)−O RDF up to the first shell border at 3.75 Å yields average coordination numbers of 6.2 (QM/MM) and 6.8 (QMCF), respectively. A broad plateau follows the first shell peak, its intensity never exceeding a value of 1.1. At the hardly detectable minimum located at 6.25 Å the intensity of the RDF is 0.9. These values indicate that the influence of the ion on the solvent beyond the first shell is extraordinarily weak and that de facto only a single hydration shell exists.

Besides the first shell distance and the coordination number the half-widths and intensity of the first shell peak are sensitive indicators to quantify hydration structures. The half-width of the first shell peak of the Na(I)−O RDF obtained from the QMCF MD simulation is 0.34 Å, and in the case of the QM/MM method a value of 0.36 Å was found. In the case of K(I) a half-width of 0.46 Å results from both simulations, indicating a higher flexibility of the first hydration shell. An accompanying decrease of the peak intensity from ∼5.3 to ∼3.2 from Na(I) to K(I) confirms this conclusion.

Hydration structures can be discussed further on the basis of angular distribution functions (ADFs). Figure 4 displays the oxygen−ion−oxygen angular distributions calculated up to the first minimum of the ion−O RDFs.

For Na(I) (see Figure 4a) the QM/MM MD simulation reveals a well-defined peak located at 90°; the QMCF method yields a peak around 85°. The lowest registered angle is approximately 50° in both cases. The probability is rising toward 180° indicating that a linear arrangement of ligands occurs. Furthermore, a distinct minimum located at 120° and 136° for the QMCF and QM/MM framework is observed. The ADF points toward an octahedron as a main structural motif, but the broad distribution as well as the minimum connecting the peaks at 90° and 180° indicate that the structure is rather flexible. The radial distribution function also reveals that ligand exchanges between first and second hydration shell occur. These migrations are connected with changes in the coordination number and an associated relaxation of the first shell structure. The lower peak intensity as well as the increased probability near the minimum found in the ADF resulting from the QMCF MD simulation indicates an increased flexibility of the hydration shell, whereas the structure is more rigid when the QM/MM framework is applied. These findings agree with the decreased first shell peaks found for the ion−hydrogen RDFs of the QM/MM simulations discussed earlier. It is important to note that the differences in the rigidity are hardly noticeable in the radial distribution functions, whereas the ADFs are highly sensitive tools to monitor these discrepancies.

In the case of K(I) both methods lead to similar ADFs (cf. Figure 4b). A weakly defined peak is visible at about 75 °, but no distinct population is observed for higher angles except a very minor increase of the intensity near 145°. However, this pattern is hardly recognizable within the fluctuation of the ADF at a mean value of 1, which indicates a disordered hydration without any preferential arrangement. The lowest registered angle in both methods was found at approximately 43°. Due to

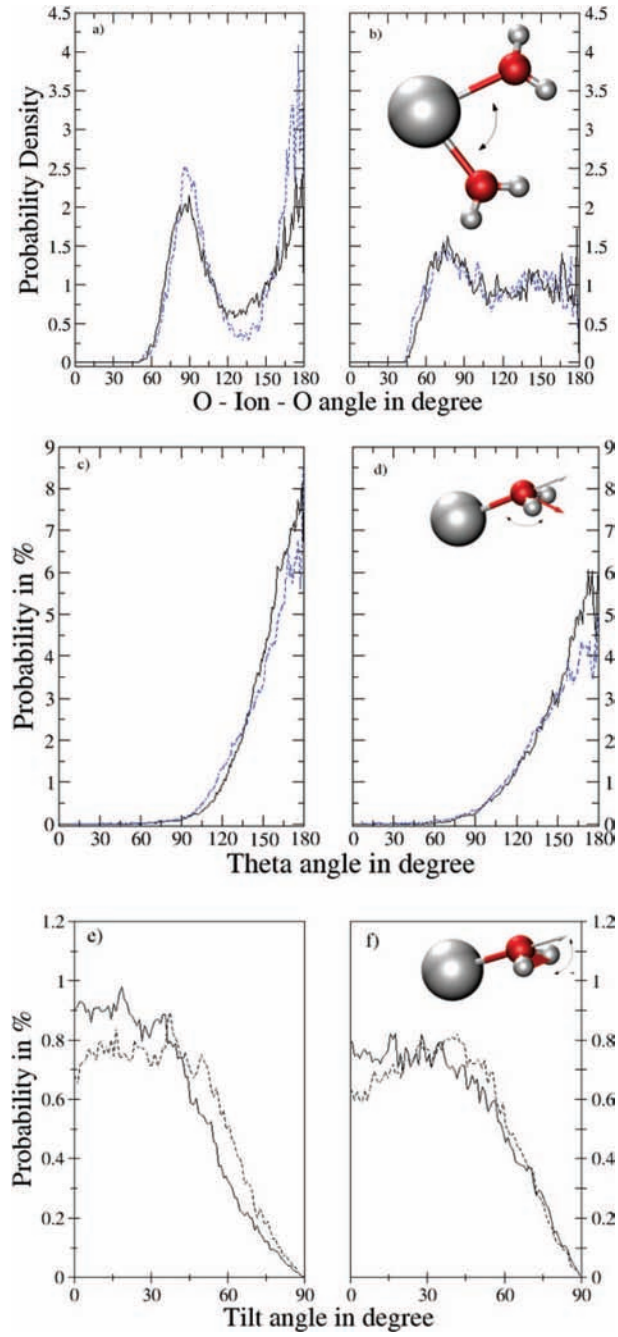

Figure 4. Comparison of the distribution of the O−ion−O angle, the θ angle, and the tilt angle for Na(I) (panels a, c, e) and K(I) (panels b, d, e) obtained from a QMCF (solid line) and a QM/MM (dashed line) MD simulation.

the longer K(I)−O distance a larger number of ligands can populate the first hydration shell, thus resulting in lower O−ion−O angles.

Besides the possibility to compare different methodical approaches, these plots are sensitve tools to quantify the differences in the hydration of the investigated ions. Na(I) forms a distinct hydration with recognizable preferences for angles near 90° and 180° corresponding to an octahedral first hydration shell. The minimum between these regions as well as the strong tailing toward lower angles indicate that this structure is by no means rigid. Intershell migrations as well as ligand exchange reactions (deduced from the RDF) lead to continuous changes in the structure, hence the octahedral arrangement has to be considered as an average structural entity. The K(I) ion on the

other hand does not show symmetry in its hydration pattern. The average angle between neighboring ligands is about 75°. However, no distinct preference for an arrangement in the region between 100° and 180° can be identified, thus indicating that the hydration shell is disordered and the arrangement of the ligands is highly flexible.

The distributions of the θ angle defined as the angle between ion−O vector and the sum of both O−H vectors are depicted in Figure 4, panels c and d. A distinct dipole orientation can be deduced for both ions, which is more pronounced when the QMCF scheme is applied. As expected, water molecules in the vicinity of K(I) have more orientational freedom than ligands in the first shell of Na(I). A similar conclusion can be drawn from the Tilt-angle distributions depicted in Figure 4, panels e and f. The tilt angle is defined as the angle between the ion−O vector and the plane defined by both O−H vectors. In the case of the QMCF MD simulations the distributions of both ions have similar shapes peaking at an angle of 0°. The intensity in the case of Na(I) is higher reflecting the stronger interaction of this ion with the solvent. The distributions resulting from the QM/MM MD simulations show some significant differences for K(I): in the case of Na(I) a plateau is formed in the region between 10° and 50°, and for K(I) the distributions peaks at about 40°. This distortion of the water geometry is another indicator of the artifacts occurring in the QM/MM framework. Apparently the "stress" acting on the QM region concluded from the radial distribution function also influences the arrangement of the first shell water molecules. Thus, the entire hydrate structure including the hydrogen bonds between the first and the second shell are subject to the artificial "pressure", whereas the application of the QMCF MD does not lead to any discrepancies in the description of the radial and angular behavior. It appears noteworthy that although the radial distribution functions of K(I) do not show significant variations, the angular distributions indicate differences between the "conventional" QM/MM and the QMCF scheme and hence highlight the methodical improvements of the latter.

Taking the flexibility of hydration of these ions into account, a varying distribution of microspecies, i.e., hydrates with a different number of first shell ligands, is to be expected. Coordination number distribution (CND) plots enable the analysis of these microspecies (see Figure 3). The QM/MM and QMCF MD simulation of Na(I) indicate that 5- and 6-fold coordination dominate the hydration. Also 7-fold coordination was observed in the case of the QMCF simulation, but its occurrence is low. In the case of K(I) the coordination numbers range from four to nine, the hexa- and heptahydrates being the most populated species resulting from the QM/MM and QMCF MD simulation, respectively. These data once more reflect the weaker hydration of the K(I) ion compared to Na(I). Both ions exchange their first shell ligands within the simulation time of 12 ps thus leading to species with varying coordination numbers and, consequently, different bond lengths and angles. Experimental structure determinations suffer from the inaccessibility of such effects occurring on the picosecond scale as all results are averaged over these species distribution. The hydrate complexes probed during an experiment will thus show an average of the overall microspecies distribution.

The QMCF framework yields lower coordination numbers than the QM/MM scheme. This result agrees well with the conclusions drawn from the radial and angular distribution functions. The "stress" on the quantum mechanical region occurring in the QM/MM framework leads to a shift of ligands toward the ion, resulting in a slightly higher average coordination.

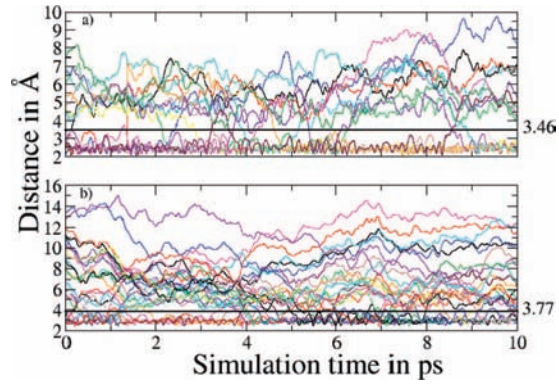

Figure 5. (a) Ion−O distances of all first shell ligands showing persisting exchanges (≥0.5 ps) obtained from the QMCF MD simulation of (a) Na(I) and (b) K(I) in aqueous solution.

Since detailed information on water exchange between hydration shells of ions and bulk is fundamental to describe the reactivity of ions, it was of special interest to evaluate the mean lifetime of the first shell ligands connected to these exchange processes. In this work, the mean residence time (MRT) values were calculated using a direct evaluation of the exchange events,[48] accepting only ligand displacements lasting longer than 0.5 ps as a successful exchange event.

The ion−oxygen distances of all first shell molecules showing lasting exchanges (≥0.5 ps) obtained from the QMCF MD simulation are depicted in panels a and b of Figure 5 for Na(I) and K(I), respectively. The first shell mean ligand residence time for Na(I) decreased from 9.7 ps in the QM/MM approach to 4.1 ps in the QMCF framework. For K(I) a similar trend was observed: the MRT of the first shell ligands decreased from 2.6 to 1.6 ps when changing from the QM/MM to the QMCF MD framework. The latter value is close to the value of pure water determined as 1.5 ps via a QM/MM MD study.[51] Taking into account the varying coordination numbers and MRT data it can be concluded that K(I) induces faster ligand movements than those occurring in the pure solvent. The Na(I)−water interaction on the other hand slows down ligand mobility compared to that of pure water. This finding appears to be important for the interpretation of the Na(I):K(I) ratio in biological fluids. It has been known for a long time that structure breakers can be utilized to denature macromolecules.[52] As K(I) leads to a slight accelaration of water molecules, whereas Na(I) stabilizes them, the ratio as well as the total concentration of these ions utilized to control the osmotic pressure can have an influence on the formation of macromolecular structures.

To address the question of whether an influence of the ion exists beyond the first hydration shell, e.g., in a rudimentary second hydration shell, an analysis of exchange events and their respective mean ligand residence times was carried out. A second shell MRT similar to that of the pure solvent (1.5 ps determined via QM/MM MD simulations)[51] would indicate that the water molecules are not influenced by the ion and hence that region has to be considered as bulk. For Na(I) values of 2.6 and 1.6 ps have been determined from the QM/MM and QMCF simulations, the corresponding values for K(I) are 1.8 and 1.4 ps, respectively. On the basis of the improved QM/MM coupling realized in the QMCF framework, data obtained from simulations utilizing this approach are considered more reliable. As expected the respective values for the second shell MRT are close to that of pure water: the deviations are due to the limits of the statistical evaluation and well within the methodical uncertainty. The extraordinary weak influence

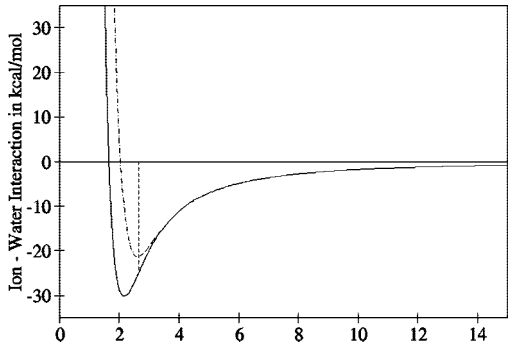

Figure 6. Ion−water interaction for Na(I) (solid line) and K(I) (dash-dotted line) computed on the CCSD/TZV level. At the minimum K(I)−H_2O distance, Na(I) interacts still stronger despite the nonoptimal distance.

of the ion beyond the first hydration shell indicated by the radial distribution function is thus confirmed on the basis of the mean lifetime of the second shell water molecules. It can be concluded that both ions are practically unable to influence the solvent beyond the first hydration shell.

The differences between Na(I) and K(I) have been recognized already from a previous MD simulation, treating only the first hydration shell by quantum mechanics.[31] On the basis of these values it was assumed that the easy desolvation of K(I) is responsible for its entrance into K-channels, and not the optimal distance of the channel's binding sites for K(I). This question was reexamined here. The QMCF-MD simulation results confirm the very loose first hydration shell of K(I), and the ion−water energy as a function of the intermolecular separation is shown in Figure 6, showing the results of ab initio potential calculations at the CCSD/TZV level. Even at the optimal K(I)−O distance, Na(I) still interacts stronger with O binding sites, but at the same time it is much harder to remove its hydration shell and hence K(I) preferentially enters the channels.

4. Conclusion

The simulation study on hydrated Na(I) and K(I) ions utilizing a "classical" QM/MM approach as well as the improved QMCF framework yielded much information. The comparison of the utilized methods has demonstrated several advantages of the QMCF methodology. The assignment of fixed partial charges to the QM atoms leads to a "pressure" on the QM region which noticeably influences the hydration characteristics. In contrast to the case of Na(I) the differences are not visible in the K(I)−water radial distribution function, whereas the angular distributions differ considerably. Ligand exchange dynamics are also subject to this artificial "stress" acting on the QM region. These shortcomings are avoided in the case of the QMCF ansatz, which incorporates the polarization of the QM region into the QM coupling by computing quantum mechanical point charges in every step of the simulation. Furthermore, the fluctuating electrostatic embedding results in a more adequate quantum mechanical treatment that further improves the QM/MM coupling. For these reasons the results deduced with the latter method appear more accurate and thus, reliable.

The QMCF MD simulation has produced results for structure and dynamics of hydrated Na(I) and K(I) which are not only in excellent agreement with available experimental data, but provide detailed insight into the nature of these essential ions in an aqueous environment.

Acknowledgment. Financial support for this work by Austrian Science Foundation (FWF) and an Austrian Technology Grant (BMWKF/RFTE) for S.S.A. are gratefully acknowledged.

References and Notes

(1) Birch, N. J.; Phillips, J. D. *Adv. Inorg. Chem.* **1991**, *36*, 49.
(2) Roux, B.; Karplus, M. *Annu. Rev. Biophys. Biomol. Struct.* **1994**, *23*, 731.
(3) Delpire, E.; Jianming, L.; England, R.; Dull, C.; Tina, T. *Nat. Genet.* **1999**, *22*, 192–195.
(4) Christian, A.; Hübner, A. B.; Thomas, J. J. *Hum. Mol. Genet.* **2002**, *11*, 2435.
(5) Rodrigo, R.; Bächler, J.; Araya, J.; Prat, H.; Passalacqua, W. *Mol. Cell. Biochem.* **2007**, *303*, 73–81.
(6) Oren, R. M. *Am. J. Cardiol.* **2005**, *95*, 2–7.
(7) Alfonzo, A. V.; Isles, C.; Geddes, C.; Deighan, C. *Resuscitation* **2006**, *70*, 10–25.
(8) Schwenk, C. F.; Tongraar, A.; Rode, B. M. *J. Mol. Liq.* **2004**, *110*, 105–122.
(9) Pálinkás, G.; Riede, W. O.; Heinzinger, K. *Z. Z. Naturforsch.* **1977**, *32*, 1137.
(10) Limtrakul, J. P.; Probst, M. M.; Rode, B. M. *J. Mol. Struct. (Theochem)* **1985**, *121*, 23–28.
(11) Mezei, M.; Beveridge, D. L. *J. Chem. Phys.* **1981**, *74*, 6902–6910.
(12) Lee, S. H.; Rasaiah, J. C. *J. Chem. Phys.* **1994**, *101*, 6964–6974.
(13) Lee, S. H.; Rasaiah, J. C. *J. Phys. Chem.* **1996**, *100*, 1420–1425.
(14) Obst, S.; Bradaczek, H. *J. Phys. Chem.* **1996**, *100*, 15677–15687.
(15) Brady, G. W. *J. Chem. Phys.* **1958**, *28*, 464–469.
(16) Pálinkás, G.; Radnai, T.; Hajdu, F. *Z. Naturforsch., Part A* **1980**, *35a*, 107–114.
(17) Caminiti, R.; Licheri, G.; Paschina, G.; Pinna, G. *J. Chem. Phys.* **1980**, *72*, 4552.
(18) Neilson, G. W.; Skipper, N. T. *Chem. Phys. Lett.* **1985**, *114*, 35–38.
(19) Skipper, N. T.; Neilson, G. W. *J. Phys.: Condens. Matter* **1989**, *1*, 4141–4154.
(20) Neilson, G. W.; Enderby, J. E. *Adv. Inorg. Chem.* **1989**, *34*, 195–218.
(21) Neilson, G. W.; Tromp, R. H. *Annu. Rev. Phys. Chem.* **1991**, *88*, 45–75.
(22) Mancinelli, R.; Botti, A.; Bruni, F.; Ricci, M. A.; Soper, A. *Phys. Chem. Chem. Phys.* **2007**, *9*, 2959–2967.
(23) Mancinelli, R.; Botti, A.; Bruni, F.; Ricci, M. A. *Phys. Chem. Chem. Phys.* **2007**, *111*, 13570–13577.
(24) Lin, H.; Truhlar, D. G. *Theor. Chem. Acc.* **2007**, *117*, 185.
(25) Warshel, A.; Levitt, M. *J. Mol. Biol.* **1976**, *103*, 227.
(26) Field, M. J.; Bash, P. A.; Karplus, M. *J. Comput. Chem.* **1990**, *11*, 700–733.
(27) Gao, J. *J. Am. Chem. Soc.* **1993**, *115*, 2930–2935.
(28) Bakowies, D.; Thiel, W. *J. Phys. Chem.* **1996**, *100*, 10580–10594.
(29) Rode, B. M.; Hofer, T. S.; Randolf, B. R.; Schwenk, C. F.; Xenides, D.; Vchirawongkwin, V. *Theor. Chem. Acc.* **2006**, *115*, 77.
(30) Hofer, T. S.; Randolf, B. R.; Rode, B. M. Chapter Molecular Dynamics Simulation Methods including Quantum Effects. In *Solvation Effects on Molecules and Biomolecules*; Canuto, S., Ed.; Springer: Heidelberg, 2008; Vol. 6.
(31) Tongraar, A.; Liedl, K. R.; Rode, B. M. *J. Chem. Phys.* **1998**, *102*, 10340–10347.
(32) Fatmi, M. Q.; Hofer, T. S.; Randolf, B. R.; Rode, B. M. *J. Chem. Phys.* **2005**, *123*, 4514–4521.
(33) Hofer, T. S.; Pribil, A. B.; Randolf, B. R.; Rode, B. M. *Chem. Phys.* **2008**, *349*, 182–185.
(34) Schwenk, C. F.; Hofer, T. S.; Rode, B. M. *J. Phys. Chem. A* **2004**, *108*, 1509.
(35) Schwenk, C. F.; Löffler, H. H.; Rode, B. M. *J. Chem. Phys.* **2001**, *115*, 10808.
(36) Schwenk, C. F.; Rode, B. M. *J. Chem. Phys.* **2003**, *119*, 9523.
(37) Hofer, T. S.; Randolf, B. R.; Rode, B. M. *Phys. Chem. Chem. Phys.* **2005**, *7*, 1382.
(38) Hofer, T. S.; Randolf, B. R.; Rode, B. M. *J. Comput. Chem.* **2005**, *26*, 949.
(39) Hofer, T. S.; Rode, B. M. *J. Chem. Phys.* **2004**, *121*, 6406.
(40) Hofer, T. S.; Rode, B. M.; Randolf, B. R. *Chem. Phys.* **2005**, *312*, 81.
(41) Hofer, T. S.; Pribil, A. B.; Randolf, B. R.; Rode, B. M. *J. Am. Chem. Soc.* **2005**, *127*, 14231.
(42) Hofer, T. S.; Scharnagl, H.; Randolf, B. R.; Rode, B. M. *Chem. Phys.* **2006**, *327*, 31.
(43) Hofer, T. S.; Randolf, B. R.; Rode, B. M. *J. Phys. Chem. B* **2006**, *110*, 20409.
(44) Hofer, T. S.; Shah, S. A. A.; Randolf, B. R.; Rode, B. M.; Persson, I. *Chem. Phys. Lett.* **2007**, *445*, 193–197.
(45) Rode, B. M.; Hofer, T. S. *Pure Appl. Chem.* **2006**, *78*, 525–539.
(46) Stillinger, F. H.; Rahman, A. *J. Chem. Phys.* **1978**, *68*, 666–670.

(47) Bopp, P.; Jansco, G.; Heinzinger, K. *Chem. Phys. Lett.* **1983**, *98*, 129–133.
(48) Hofer, T. S.; Tran, H. T.; Schwenk, C. F.; Rode, B. M. *J. Comput. Chem.* **2004**, *125*, 211–217.
(49) Berendsen, H. J.; Grigera, J. R.; Straatsma, T. P. *J. Phys. Chem.* **1987**, *91*, 6269–6271.
(50) Hofer, T. S.; Rode, B. M. *Pure Appl. Chem.* **2006**, *78*, 525–539.
(51) Xenides, D.; Randolf, B. R.; Rode, B. M. *J. Chem. Phys.* **2005**, *122*, 4506.
(52) Hofmeister, F. *Arch. Exp. Pathol. Pharmacol.* **1888**, *24*, 247.

JP8093462